

SEIRS MATHEMATICAL MODEL ON STABILITY ANALYSIS OF HIV-1 CORONAVIRUS CO-INFECTION.

ABSTRACT

Mathematical modeling has enabled epidemiologist to understand best the dynamics of infectious diseases, their impact and future predictions on their transmission and existence. Deterministic Susceptible–Vaccinated–Exposed–Infectious–Recovered (SVEIR) model on HIV-1 Coronavirus co-infection was formulated based on piecewise linear dynamical systems with constant delay. Delay here accounts for the time lapse between exposure and when the symptoms of the disease appear. Basic reproduction number R_0 is the threshold parameter on which the growth or reduction of the disease is based and calculated using Next Generation Matrix approach. Disease Free Equilibrium is attained when reproduction number is less or equals to one. The Disease Free Equilibrium is globally asymptotically stable whenever the reproductive number is less or equal to one and unstable otherwise and it is showed using Lyapunov function. Numerical simulation is performed using Matrix Laboratory (MatLab) dde23 solver to authenticate the analytic results. Graphical representation is then done so as to highlight on future disease dynamics and interventions. Time-delay, vaccination and chemotherapy plays a major role in stabilizing disease free equilibrium.

Keywords: Coronavirus, Basic reproduction number, Global stability, Lyapunov's function.

1. Introduction

There is a widespread concern worldwide over the emergence of new infectious disease that have wrecked havoc on human population. Human immunodeficiency virus 1 (HIV-1) and coronavirus disease are infectious diseases that have been of great concern to both scientists and medical practitioners in the recent past. The main purpose of this study was to investigate the impacts of protection with quarantine, CoVid-19 vaccination, HIV-1 and CoVid-19 chemotherapy, controlling and prevention strategies on transmission dynamics of HIV-1 and AIDs and CoVid-19 co-infection. A mathematical modeling approach was thus used in which a deterministic Susceptible-Vaccinated-Exposed-Infected-Removed (SVEIR) HIV-1 Covid-19 co-infection model was formulated. The model considers the time lag that occurs between exposure of the Coronavirus disease and when the disease appears and its effects. Delay differential equations (DDEs) with constant delay were formulated. [4,5,12,15,33,34]

According to [8,9,17,26,29]) HIV and COVID-19 co-infection model with ABC-fractional operator approach was formulated to investigate an epidemic prediction of combined HIV-COVID-19 co-infection. Numerical simulations carried out established that the disease would stabilize at a later stage when enough protection strategies are taken. A mathematical model on

HIV and COVID-19 co-infection with optimal control strategies were formulated and analyzed by [14, 27, 30, 31]. The analysis suggested that COVID-19 only prevention strategy is the most effective strategy and it averted about 10,500 new co-infection cases. Further, [2, 3, 22,24,25] studied analysis of COVID-19 and comorbidity specifically diabetes mellitus co-infection model with optimal control. The model showed backward bifurcation caused by parameter accounting for susceptibility for Covid-19 and rate of reinfection. According to [1,11,20,32]they constructed and examined HIV/AIDS and Pneumonia co-infection model with control measures such as pneumonia vaccination and treatment of pneumonia and HIV/AIDS infections. Numerical simulations on the model showed that pneumonia treatment and vaccination played a major role in reducing pneumonia and co-epidemic disease growth while at the same time decreasing the growth rate of HIV infection to the AIDS stage. A mathematical model for cholera and COVID-19 co-infection which describes the transmission dynamics of COVID-19 and cholera in Yemen was studiedby [18,20,21,23]. The results showed that preventive measures such as number of chlorine water tablets, lockdown, social distancing and number of tests played a key role in reducing spread of the disease. COVID-19 and tuberculosis co-dynamics model with optimal control strategies carried out by [6,14,19,25] suggested that COVID-19 prevention, treatment and control of co-infection yields a better outcome in terms in terms of the number of COVID-19 cases prevented at a lower percentage of the total cost of this strategy. Ordinary differential equationsconstructed by [7, 10,13, 16]modeled Bifurcation and optimal control analysis of HIV/AIDS and COVID-19 co-infection model with numerical simulation. The main purpose of this paper was to investigate the impacts of COVID-19 protection with quarantine, COVID-19 treatment, HIV protection and HIV treatment prevention and controlling strategies on the transmission dynamics of HIV/AIDS and COVID-19 co-infection in the community with mathematical approach. The R_0 value of the SQEIRP model is 3.78, meaning that one patient can lead to approximately three additional infections.

In this study, a deterministic SVEIR HIV-1 Coronavirus co-infection model was formulated to take into account the time lag that occurs between the exposure of a Coronavirus disease and its effects. Delay differential equations DDEs with constant delay were formulated. Local and global stability of disease free equilibrium, bifurcation analysis and type of bifurcation were taken into account.

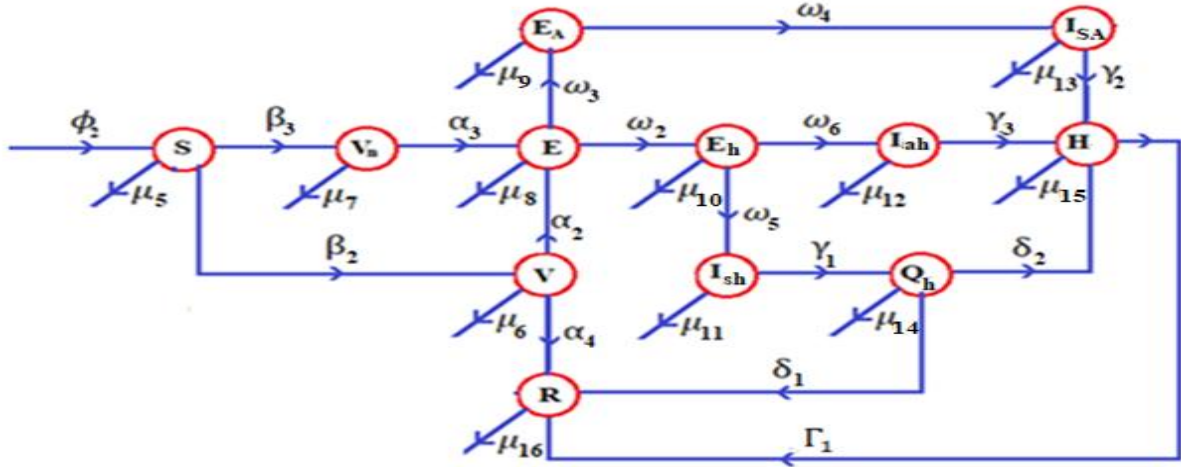
2. Methodology

In the study, the total population were partitioned into twelve mutually-exclusive compartments basing on their infection status: susceptible class to both HIV-1 and Coronavirus disease (S), individuals vaccinated against Coronavirus disease (V), individuals not vaccinated against Coronavirus disease (V_n), Exposed class (E), Exposed class with HIV-1 (E_h), Exposed class with AIDs (E_A), symptomatic infected individuals with AIDs (I_{SA}), symptomatic infected class with HIV-1 (I_{Sh}), asymptomatic infected class with HIV-1 (I_{ah}), Quarantined class with HIV-1 (Q_h), Hospitalized class (H) and Removed class (R). Other parameters considered are:

Recruitment rate (ϕ_2), rate of progression from S to V (β_3), Rate of progression from S to V_n (β_4), Rate of progression from V to E (α_3), Rate of progression from V_n to E (α_4), Rate of progression from V to R (α_5), Rate of progression from E to E_h (ω_3), Rate of progression from E to E_A (ω_4), Rate of progression from E_A to I_{SA} (ω_5), Rate of progression from E_h to I_{Sh} (ω_6), Rate of progression from E_h to I_{ah} (ω_7), Rate of progression from H to R (γ_2), Rate of progression from I_{Sh} to Q_n (γ_3), Rate of progression from I_{SA} to H (γ_4), Rate of progression from

I_{ah} to $H(\gamma_5)$, Rate of progression from Q_h to $R(\delta_4)$, Rate of progression from Q_h to $H(\delta_5)$, Natural death rate (μ) and time delay (τ).

Figure 1: SVEIR CO-INFECTION MODEL



$$\frac{dS}{dt} = \phi_2 - \mu_5 S - \beta_2 S - \beta_3 S$$

$$\frac{dV}{dt} = \beta_2 S - \mu_6 V - \alpha_2 V_\tau - \alpha_4 V_\tau$$

$$\frac{dV_n}{dt} = \beta_3 S - \mu_7 V_n - \alpha_3 V_{n\tau}$$

$$\frac{dE}{dt} = \alpha_2 V_\tau + \alpha_3 V_{n\tau} - \mu_8 E - \omega_2 E_\tau - \omega_3 E_\tau$$

$$\frac{dE_A}{dt} = \omega_3 E_\tau - \mu_9 E_A - \omega_4 E_{A\tau}$$

$$\frac{dE_h}{dt} = \omega_2 E_\tau - \mu_{10} E_h - \omega_5 E_{h\tau} - \omega_6 E_{h\tau} \text{ System 1 (*)}$$

$$\frac{dI_{sh}}{dt} = \omega_5 E_{h\tau} - \mu_{11} I_{sh} - \gamma_1 I_{sh\tau}$$

$$\frac{dI_{ah}}{dt} = \omega_6 E_{h\tau} - \mu_{12} I_{ah} - \gamma_2 I_{ah\tau}$$

$$\frac{dI_{SA}}{dt} = \omega_4 E_{A\tau} - \mu_{13} I_{SA} - \gamma_3 I_{SA\tau}$$

$$\frac{dQ_h}{dt} = \gamma_1 I_{sh\tau} - \delta_1 Q_{h\tau} - \delta_2 Q_{h\tau} - \mu_{14} Q_h$$

$$\frac{dH}{dt} = \gamma_2 I_{SA\tau} + \gamma_3 I_{ah\tau} + \delta_2 Q_{h\tau} - \mu_{15} H - \Gamma_1 H_\tau$$

$$\frac{dR}{dt} = \delta_1 Q_{h\tau} + \Gamma_1 H_\tau + \alpha_4 V_\tau - \mu_{16} R$$

2.1 Model Preliminary Analysis

2.1.1 Properties of Solutions of the Model

Positivity and boundedness of the model is shown before doing result analysis for biological reasons. Transformation of population of cell is well elaborated such that cell numbers remain positive and bounded and existence of solutions are underscored by these properties.

Let's define a positive quadrant space $C = C^1([- \tau, 0]; \mathbb{R}^{12})$ equipped with the norm $\|\Phi\| = \sup \Phi(t)_{t \in [-\tau, 0]}$ as a Banach space of continuous functions mapping the $[-\tau, 0]$ into \mathbb{R}^{12} with the topology of uniform convergence. Let the positive initial conditions of system 1 (*) at a time $t = t_0$ be

$S(t_0) = S_0 \geq 0, V(t_0) = V_0 \geq 0, (V_n(t_0) = V_{n_0} \geq 0, E(t_0) = E_0 \geq 0, E_A(t_0) = E_{A_0} \geq 0, E_h(t_0) = E_{h_0} \geq 0, I_{sh}(t_0) = I_{sh_0} \geq 0, I_{ah}(t_0) = I_{ah_0} \geq 0, I_{sA}(t_0) = I_{sA_0} \geq 0, Q_h(t_0) = Q_{h_0} \geq 0, H_h(t_0) = H_{h_0} \geq 0, R(t_0) = R_0 \geq 0, t_0 \in [-\tau, 0]$ In this case, we define a positive quadrant space of solutions as

$$\mathbb{R}_{+0} = \{(S, V, V_n, E, E_A, E_h, I_{sh}, I_{ah}, I_{sA}, Q_h, H_h, R) | S \geq 0, V \geq 0, V_n \geq 0, E \geq 0, E_A \geq 0, E_h \geq 0, I_{sh} \geq 0, I_{ah} \geq 0, I_{sA} \geq 0, Q_h \geq 0, H_h \geq 0, R \geq 0\} \quad 2$$

$$\mathbb{R}_+ = \{(S, V, V_n, E, E_A, E_h, I_{sh}, I_{ah}, I_{sA}, Q_h, H_h, R) | S > 0, V > 0, V_n > 0, E > 0, E_A > 0, E_h > 0, I_{sh} > 0, I_{ah} > 0, I_{sA} > 0, Q_h > 0, H_h > 0, R > 0\} \quad 3$$

By fundamental theory of differential equations it can be shown that there exists a unique solution $(S(t), V(t), V_n(t), E(t), E_A(t), E_h(t), I_{sh}(t), I_{ah}(t), I_{sA}(t), Q_h(t), H_h(t), R(t))$ of the system 1(*) with initial data in \mathbb{R}_+ as follows:

From system 1 (*), by integrating we have

$$s(t) = S(0)e^{\int_0^t (\mu_5 + \beta_2 + \beta_3) d\eta} + \int_0^t (\phi_1 + (\mu_5 + \beta_2 + \beta_3)) S(\xi) e^{\int_0^t (\mu_5 + \beta_2 + \beta_3) d\eta} d\xi \quad 4$$

From (4) it's clearly seen that $S(t) > 0$ hence positive.

Similarly, it can be shown that

$$(V(t) > 0, V_n(t) > 0, E(t) > 0, E_A(t) > 0, E_h(t) > 0, I_{sh} > 0, I_{ah} > 0, I_{sA} > 0, Q_h > 0, H_h > 0, R > 0) \quad 5$$

Using (4) positivity immediately follows from the above integral forms.

For boundedness we define;

$$N(t) = S(t) + V(t) + V_n(t) + E(t) + E_A(t) + E_h(t) + I_{sh}(t) + I_{ah}(t) + I_{sA}(t) + Q_h(t) + H_h(t) + R(t) \quad 6$$

$$\frac{dN(t)}{dt} = \frac{d(S(t) + V(t) + V_n(t) + E(t) + E_A(t) + E_h(t) + I_{sh}(t) + I_{ah}(t) + I_{sA}(t) + Q_h(t) + H_h(t) + R(t))}{dt} \quad 7$$

Thus,

$$\frac{dN(t)}{dt} \leq \Phi_2 - \sum \mu. \text{ Where } \sum \mu = \mu_1 + \mu_2 + \dots + \mu_{12}.$$

8

This implies that $N(t)$ is bounded and so

$$(S(t), V(t), V_n(t), E(t), E_A(t), E_h(t), I_{sh}(t), I_{ah}(t), I_{sA}(t), Q_h(t), H(t), R(t)).$$

2.3 Computation of Basic Reproductive Number R_0

Figure 1: HIV-1 Coronavirus co-infection model

In system 1 there are seven infection classes: $E, E_A, E_h, I_{sh}, I_{ah}, I_{sA}, Q_h$. Therefore, at disease free equilibrium (DFE) the matrix of new infection is given by matrices F and V .

$$\mathcal{F}_i = \begin{bmatrix} (\omega_2 + \omega_3)E_\tau \\ \omega_4 E_{A\tau} \\ (\omega_5 + \omega_6)E_{h\tau} \\ \gamma_1 I_{sh\tau} \\ \gamma_2 I_{ah\tau} \\ \gamma_3 I_{sA\tau} \\ \delta_2 Q_{h\tau} \end{bmatrix} \quad \mathcal{V}_i = \begin{bmatrix} -\mu_8 E \\ -\mu_9 E_A \\ -\mu_{10} E_h \\ -\mu_{11} I_{sh} \\ -\mu_{12} I_{ah} \\ -\mu_{13} I_{sA} \\ \delta_2 Q_{h\tau} - \mu_{14} Q_h \end{bmatrix}$$

Differentiating partially with respect to state variables we have:

$$F = \begin{bmatrix} (\omega_2 + \omega_3)e^{-\lambda\tau} & 0 & 0 & 0 & 0 & 0 & 0 \\ 0 & \omega_4 e^{-\lambda\tau} & 0 & 0 & 0 & 0 & 0 \\ 0 & 0 & (\omega_5 + \omega_6)e^{-\lambda\tau} & 0 & 0 & 0 & 0 \\ 0 & 0 & 0 & \gamma_1 e^{-\lambda\tau} & 0 & 0 & 0 \\ 0 & 0 & 0 & 0 & \gamma_2 e^{-\lambda\tau} & 0 & 0 \\ 0 & 0 & 0 & 0 & 0 & \gamma_3 e^{-\lambda\tau} & 0 \\ 0 & 0 & 0 & 0 & 0 & 0 & \delta_2 e^{-\lambda\tau} \end{bmatrix}$$

$$V = \begin{bmatrix} -\mu_8 & 0 & 0 & 0 & 0 & 0 & 0 \\ 0 & -\mu_9 & 0 & 0 & 0 & 0 & 0 \\ 0 & 0 & -\mu_{10} & 0 & 0 & 0 & 0 \\ 0 & 0 & 0 & -\mu_{11} & 0 & 0 & 0 \\ 0 & 0 & 0 & 0 & -\mu_{12} & 0 & 0 \\ 0 & 0 & 0 & 0 & 0 & -\mu_{13} & 0 \\ 0 & 0 & 0 & 0 & 0 & 0 & \delta_1 e^{-\lambda\tau} - \mu_{14} \end{bmatrix}$$

$$V^{-1} = \begin{bmatrix} -\frac{1}{\mu_8} & 0 & 0 & 0 & 0 & 0 & 0 & 0 \\ 0 & -\frac{1}{\mu_9} & 0 & 0 & 0 & 0 & 0 & 0 \\ 0 & 0 & -\frac{1}{\mu_{10}} & 0 & 0 & 0 & 0 & 0 \\ 0 & 0 & 0 & -\frac{1}{\mu_{11}} & 0 & 0 & 0 & 0 \\ 0 & 0 & 0 & 0 & -\frac{1}{\mu_{12}} & 0 & 0 & 0 \\ 0 & 0 & 0 & 0 & 0 & -\frac{1}{\mu_{13}} & 0 & 0 \\ 0 & 0 & 0 & 0 & 0 & 0 & -\frac{1}{\delta_2 e^{-\lambda\tau} - \mu_{14}} & 0 \end{bmatrix}$$

$$FV^{-1} = \begin{bmatrix} -\frac{(\omega_2 + \omega_3)e^{-\lambda\tau}}{\mu_8} & 0 & 0 & 0 & 0 & 0 & 0 & 0 \\ 0 & -\frac{\omega_4 e^{-\lambda\tau}}{\mu_9} & 0 & 0 & 0 & 0 & 0 & 0 \\ 0 & 0 & -\frac{(\omega_5 + \omega_6)e^{-\lambda\tau}}{\mu_{10}} & 0 & 0 & 0 & 0 & 0 \\ 0 & 0 & 0 & -\frac{\gamma_1 e^{-\lambda\tau}}{\mu_{11}} & 0 & 0 & 0 & 0 \\ 0 & 0 & 0 & 0 & -\frac{\gamma_2 e^{-\lambda\tau}}{\mu_{12}} & 0 & 0 & 0 \\ 0 & 0 & 0 & 0 & 0 & -\frac{\gamma_3 e^{-\lambda\tau}}{\mu_{13}} & 0 & 0 \\ 0 & 0 & 0 & 0 & 0 & 0 & 0 & -\frac{\delta_1 e^{-\lambda\tau}}{\delta_2 e^{-\lambda\tau} - \mu_{14}} \end{bmatrix}$$

To find the eigenvalues we have;

$$\begin{array}{cccccccc}
-\frac{(\omega_2 + \omega_3)e^{-\lambda\tau}}{\mu_8} - \lambda & 0 & 0 & 0 & 0 & 0 & 0 & 0 \\
0 & -\frac{\omega_4 e^{-\lambda\tau}}{\mu_9} - \lambda & 0 & 0 & 0 & 0 & 0 & 0 \\
0 & 0 & -\frac{(\omega_5 + \omega_6)e^{-\lambda\tau}}{\mu_{10}} - \lambda & 0 & 0 & 0 & 0 & 0 \\
0 & 0 & 0 & -\frac{\gamma_1 e^{-\lambda\tau}}{\mu_{11}} - \lambda & 0 & 0 & 0 & 0 \\
0 & 0 & 0 & 0 & -\frac{\gamma_2 e^{-\lambda\tau}}{\mu_{12}} - \lambda & 0 & 0 & 0 \\
0 & 0 & 0 & 0 & 0 & -\frac{\gamma_3 e^{-\lambda\tau}}{\mu_{13}} - \lambda & 0 & 0 \\
0 & 0 & 0 & 0 & 0 & 0 & 0 & -\frac{\delta_1 e^{-\lambda\tau}}{\delta_2 e^{-\lambda\tau} - \mu_{14}} - \lambda
\end{array}
= 0$$

Solving for eigenvalues we obtain;

$$\lambda_1^* = -\frac{(\omega_2 + \omega_3)e^{-\lambda\tau}}{\mu_8}$$

$$\lambda_2^* = -\frac{\omega_4 e^{-\lambda\tau}}{\mu_9}$$

$$\lambda_3^* = -\frac{(\omega_5 + \omega_6)e^{-\lambda\tau}}{\mu_{10}}$$

$$\lambda_4^* = -\frac{\gamma_1 e^{-\lambda\tau}}{\mu_{11}}$$

$$\lambda_5^* = -\frac{\gamma_2 e^{-\lambda\tau}}{\mu_{12}}$$

$$\lambda_6^* = -\frac{\gamma_3 e^{-\lambda\tau}}{\mu_{13}}$$

$$\lambda_7^* = -\frac{\delta_1 e^{-\lambda\tau}}{\delta_2 e^{-\lambda\tau} - \mu_{14}}$$

The dominant eigenvalue is

$$\lambda_7^* = -\frac{\delta_1 e^{-\lambda\tau}}{\delta_2 e^{-\lambda\tau} - \mu_{14}}$$

Therefore, $R_{0(model\ 2.1)} = \lambda_7^* = -\frac{\delta_1 e^{-\lambda\tau}}{\delta_2 e^{-\lambda\tau} - \mu_{14}}$

2.4 Disease Free Equilibrium Point and its Stability

To clearly understand the dynamics of HIV-1 Coronavirus co infection progresses, we study the stability of figure 1. Mathematical epidemiology considers two equilibria points, Disease Free Equilibrium Point (DFE) and Endemic Equilibrium Point (EEP). In this study we analyzed disease free equilibrium point of the system 1 and studied their stabilities. An equilibrium point is attained by setting the right handside of each equation of system1 to zero, then solving each equation algebraically for the constant solution.

Disease free equilibrium point is a viable region in the solution of system1 in absence of viral infection and co infection. For our model, we see that DFE is set of $(S^0, V^0, V_n^0, E^0, E_A^0, E_h^0, I_{sh}^0, I_{ah}^0, I_{SA}^0, Q_h^0, H^0, R^0) = (\frac{\phi_2}{\sum \mu}, 0, 0, 0, 0, 0, 0, 0, 0, 0, 0, 0)$ for figure1 obtained by simple algebraic computation in the absence of viruses.

2.4.1 Stability of Disease Free Equilibrium

The disease free equilibrium is the state of variable of the model in the absence of disease. Its stability can be tested using the eigenvalues of Jacobian matrix obtained at DFE, where at this point reproduction number is less than one. The linearization matrix of system1 is given by:

$$\begin{pmatrix} -\mu_5 - \beta_2 - \beta_3 & 0 & 0 & 0 & 0 & 0 & 0 & 0 & 0 & 0 & 0 & 0 & 0 & 0 & 0 & 0 \\ \beta_2 & -\mu_6 - \alpha_2 e^{-\lambda\tau} - \alpha_4 e^{-\lambda\tau} & 0 & 0 & 0 & 0 & 0 & 0 & 0 & 0 & 0 & 0 & 0 & 0 & 0 & 0 \\ \beta_3 & 0 & -\mu_7 - \alpha_3 e^{-\lambda\tau} & 0 & 0 & 0 & 0 & 0 & 0 & 0 & 0 & 0 & 0 & 0 & 0 & 0 \\ 0 & \alpha_2 e^{-\lambda\tau} & \alpha_3 e^{-\lambda\tau} & -\mu_8 - \omega_2 e^{-\lambda\tau} - \omega_3 e^{-\lambda\tau} & 0 & 0 & 0 & 0 & 0 & 0 & 0 & 0 & 0 & 0 & 0 & 0 \\ 0 & 0 & 0 & \omega_3 e^{-\lambda\tau} & -\mu_9 - \omega_4 e^{-\lambda\tau} & 0 & 0 & 0 & 0 & 0 & 0 & 0 & 0 & 0 & 0 & 0 \\ 0 & 0 & 0 & \omega_2 e^{-\lambda\tau} & \omega_5 e^{-\lambda\tau} & -\mu_{10} - \omega_5 e^{-\lambda\tau} - \omega_6 e^{-\lambda\tau} & 0 & 0 & 0 & 0 & 0 & 0 & 0 & 0 & 0 & 0 \\ 0 & 0 & 0 & 0 & 0 & \omega_5 e^{-\lambda\tau} & -\mu_{11} - \gamma_1 e^{-\lambda\tau} & 0 & 0 & 0 & 0 & 0 & 0 & 0 & 0 & 0 \\ 0 & 0 & 0 & 0 & 0 & \omega_6 e^{-\lambda\tau} & 0 & -\mu_{12} - \gamma_2 e^{-\lambda\tau} & 0 & 0 & 0 & 0 & 0 & 0 & 0 & 0 \\ 0 & 0 & 0 & 0 & \omega_4 e^{-\lambda\tau} & 0 & 0 & 0 & -\mu_{13} - \gamma_3 e^{-\lambda\tau} & 0 & 0 & 0 & 0 & 0 & 0 & 0 \\ 0 & 0 & 0 & 0 & 0 & 0 & \gamma_1 e^{-\lambda\tau} & 0 & 0 & -\delta_1 e^{-\lambda\tau} - \delta_2 e^{-\lambda\tau} - \mu_{14} & 0 & 0 & 0 & 0 & 0 \\ 0 & 0 & 0 & 0 & 0 & 0 & 0 & \gamma_3 e^{-\lambda\tau} & \gamma_2 e^{-\lambda\tau} & \delta_2 e^{-\lambda\tau} & -\mu_{15} & -\Gamma_1 e^{-\lambda\tau} & 0 & 0 & 0 & 0 \\ 0 & 0 & \alpha_4 e^{-\lambda\tau} & 0 & 0 & 0 & 0 & 0 & 0 & \delta_1 e^{-\lambda\tau} & \Gamma_1 e^{-\lambda\tau} & -\mu_{16} & -\Gamma_1 e^{-\lambda\tau} & -\mu_{16} & 0 & 0 \end{pmatrix}$$

The system 1(*) is locally asymptotically stable if all the eigenvalues of linearization matrix of system1 are negative. Clearly, the eigenvalues are:

$$\begin{aligned} \lambda_1^{**} &= -(\mu_5 + \beta_2 + \beta_3) \\ \lambda_2^{**} &= -(\mu_6 + (\alpha_2 + \alpha_4)e^{-\lambda\tau}) \\ \lambda_3^{**} &= -\mu_7 - \alpha_3 e^{-\lambda\tau} \\ \lambda_4^{**} &= -(\mu_8 + (\omega_2 + \omega_3)e^{-\lambda\tau}) \\ \lambda_5^{**} &= -\mu_9 - \omega_4 e^{-\lambda\tau} \\ \lambda_6^{**} &= -(\mu_{10} + (\omega_5 + \omega_6)e^{-\lambda\tau}) \\ \lambda_7^{**} &= -\mu_{11} - \gamma_1 e^{-\lambda\tau} \\ \lambda_8^{**} &= -\mu_{12} - \gamma_2 e^{-\lambda\tau} \\ \lambda_9^{**} &= -\mu_{13} - \gamma_3 e^{-\lambda\tau} \\ \lambda_{10}^{**} &= -\mu_{14} + ((\delta_1 + \delta_2)e^{-\lambda\tau}) \\ \lambda_{11}^{**} &= -\mu_{15} - \Gamma_1 e^{-\lambda\tau} \\ \lambda_{12}^{**} &= -\mu_{16} \end{aligned}$$

For model 1; it's clear that the dominant eigenvalue is

$$\lambda_{10}^{**} = -\mu_{14} + ((\delta_1 + \delta_2)e^{-\lambda\tau})$$

Theorem 1.

Disease free equilibrium is stable whenever $R_0 < 1$ otherwise unstable.

Proof

λ_{10}^{**} should be negative. This can only be negative if;

$$\delta_1 e^{-\lambda\tau} < \delta_2 e^{-\lambda\tau} - \mu_{14}$$

Clearly,

$$\frac{\delta_1 e^{-\lambda\tau}}{\delta_2 e^{-\lambda\tau} - \mu_{14}} < 1$$

Therefore $R_0 < 1$ is attained for DFE to be stable.

2.5 Local and Global stability analysis

2.5.1 Local stability analysis of disease free equilibrium points

Local stability of disease free equilibrium point is the point where if the system is put somewhere nearby the equilibrium point, it will move itself to the equilibrium point in some time.

2.5.2 Global stability analysis of disease free equilibrium points

Global stability of system 1(*) was done by constructing Lyapunov functions for disease free equilibrium point.

Theorem 2:

If $R_0 < 1$ then the disease free equilibrium of system 1(*) is globally asymptotically stable, otherwise unstable if $R_0 > 1$.

Proof

$$\begin{aligned} v(S, V, V_n, E, E_A, E_h, I_{sh}, I_{ah}, I_{sA}, Q_h, H_h, R) &= (S - S^0)^2 + (V - 0)^2 + \dots + (R - 0)^2 \text{ System 2} \\ &= (S - S^0)^2 + V^2 + \dots + R^2 \end{aligned}$$

From system 2

$$S = \frac{\phi_2}{\mu_5 + \beta_2 + \beta_3} \text{ implying that } S > 0 \text{ hence positive. It follows that}$$

$$V = V_n = E = \dots = R > 0$$

The time derivative of system 2 is

$$\frac{dv}{dt}(S, V, V_n, E, E_A, E_h, I_{sh}, I_{ah}, I_{sA}, Q_h, H_h, R) = 2(S - S^0) \frac{dS}{dt} + 2V \frac{dV}{dt} + \dots + 2R \frac{dR}{dt}$$

At Disease Free Equilibrium Point, $V = V_n = E = \dots = R = 0$ hence the equation above becomes $\dot{v} = 2(S - S_0)$. For global stability $S < S_0$ so that $\dot{v} < 0$. If $S \leq S_0$ then $\dot{v} \leq 0$ implying that $R_0 \leq 1$ hence the Disease Free Equilibrium Point is globally stable.

3. Main Results

Analytic solutions can be demonstrated using analytic results with specific numerical examples. The model equation (1) is considered. A numerical simulation of the model is calculated using list of parameters and their estimated values given in the table 1 & 2. The values have been obtained from [1, 7, 10]. In simulation of the model system (1), the following initial values in each compartment at the onset of infection is assumed to apply; $(S(0), V(0), V_n(0), E(0), E_A(0), E_h(0), I_{sh}(0), I_{ah}(0), I_{sA}(0), Q_h(0), H(0), R(0)) = (1000, 0, 0.01, 0.01, 500, 30, 0, 0, 0, 0, 0, 0)$ on the interval $[-\tau, 0]$.

Table 1. Table of Variable, Variable description and Value.

Parameters	Parameter description	Value	Source
S	susceptible class to both HIV-1 and Coronavirus disease (S)	2500	Fixed
V	Coronavirus disease vaccinated class (V)	1000	Estimated
V_n	Coronavirus disease non-vaccinated class (V_n)	1500	Estimated
E	Exposed class (E)	100	Estimated
E_A	Exposed class with HIV-1 (E_h)	10	Estimated
E_h	Exposed class with AIDs (E_A)	10	Estimated
I_{sA}	symptomatic infected class with AIDs (I_{sA})	0	Assumed
I_{sh}	symptomatic infected class with HIV-1 (I_{sh})	0	Assumed
I_{ah}	asymptomatic infected class with HIV-1 (I_{ah})	0	Assumed
Q_h	Quarantined class with HIV-1 (Q_h)	15	Estimated
H	Hospitalized class (H)	20	Estimated
R	Removed class (R)	5	Assumed
ϕ_2	Recruitment rate	2500	16
β_3	Rate of progression from S to V	0.20	Assumed
β_4	Rate of progression from S to V_n	0.002	14
α_3	Rate of progression from V to E	0.53	Estimated
α_4	Rate of progression from V_n to E	0.45	Estimated
α_5	Rate of progression from V to R	0.50	Estimated

ω_3	Rate of progression from E to E_h	0.4	Estimated
ω_4	Rate of progression from E to E_A	0.05	Estimated
ω_5	Rate of progression from E_A to I_{SA}	0.043	Estimated
ω_6	Rate of progression from E_h to I_{Sh}	0.045	Estimated
ω_7	Rate of progression from E_h to I_{ah}	0.3425	Estimated
γ_2	Rate of progression from H to R	0.05	22
γ_3	Rate of progression from I_{Sh} to Q_n	0.3	16
γ_4	Rate of progression from I_{SA} to H	0.3	16
γ_5	Rate of progression from I_{ah} to H	0.38	16
δ_4	Rate of progression from Q_h to R	0.200	22
δ_5	Rate of progression from Q_h to H	0.3	Assumed
μ	Natural death rate	$0.019 < \mu < 0.51$	16

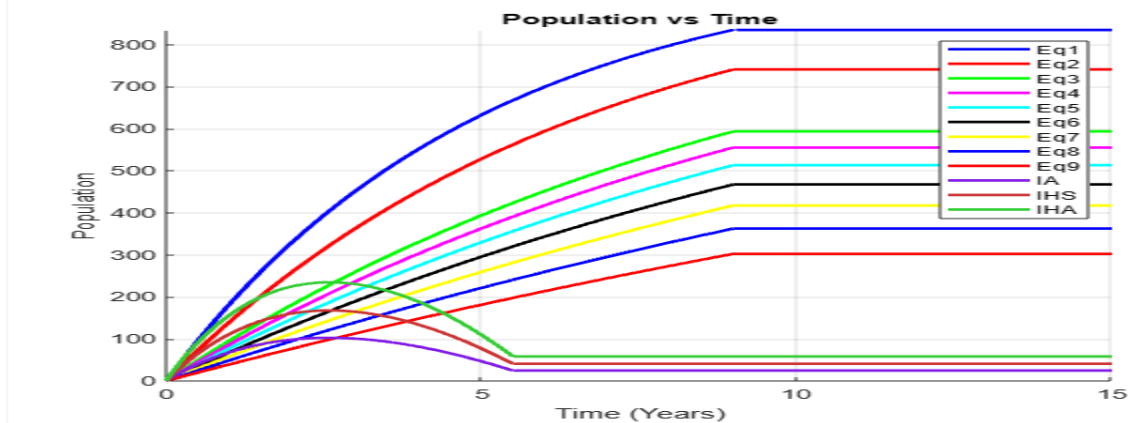


Figure 2. population vs time

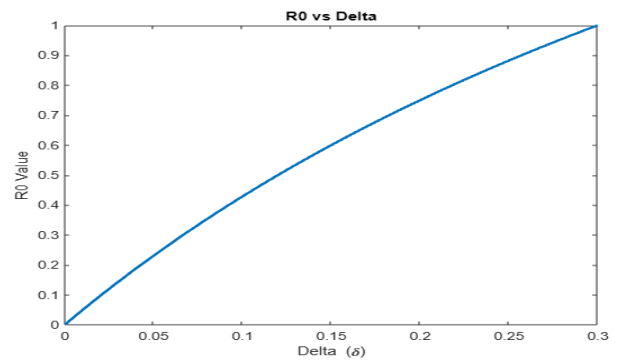
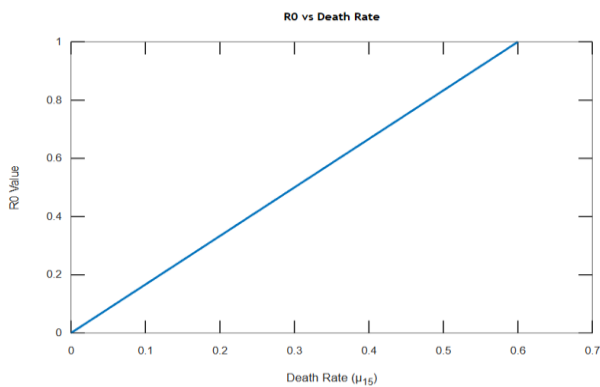


Figure 3. RO vs death rate

Figure 4.RO vs delta

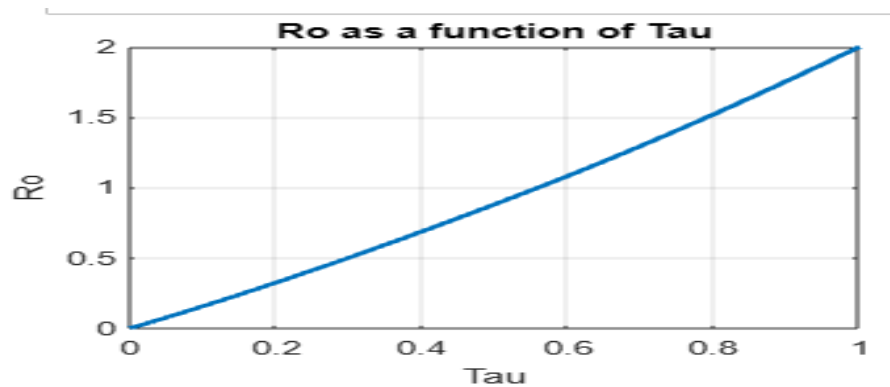


Figure 5. Ro as a function of Tau

Discussion

Numerical results showed that death rate, time lag, vaccination and quarantine affected the growth of the disease as it is seen from reproduction number. Figure 2 shows cell population with time, clearly the infected individuals curve were at zero initially then it increases steadily, it then reduces after some time when interventions like vaccination, quarantine and treatment were put in place. Further, the curve for susceptible individuals rises steadily and stabilizes at higher value than the other curves. Figures 3, 4 and 5 show how reproduction number is affected by death rate, quarantine and time lag respectively. When death rate and number of individuals being taken to quarantine is high then it means that the disease is growing. When time lag is 0.56days then the reproduction number is less than one and it means the disease is dying out.

Conclusion

Disease Free Equilibrium is attained when $R_0 < 1$. This is affected by vaccination, time delay, quarantine and chemotherapy of both HIV-1 and CoVid-19. The study found out that if all other factors are kept constant then DFE is achieved when drug efficacy is above fifty percent. It is also clear that for $\tau > 0$ DFE is stable and unstable otherwise.

References

1. Ahmed Idris, D. G. (2021). An epidemic prediction from analysis of a combined HIV-COVID-19 co-infection model via ABC-fractional operator. *Alexandria Engineering Journal* 60, 2979-2995.
2. Ali Alarjani, M. T. (2020). Application of Mathematical modelling in prediction of COVID-19 transmission dynamics . *Journal of computer engineering and computer science, Springer open publishers*.
3. Anwar Zeb, E. A. (2020). SEIQR model for coronavirus disease 2019 containing isolation class. *Journal of Biomed Research International Hindawi Publishers*, 7 pages.
4. Batra, A., Swaby, J., Raval, P., Zhu, H., Weintraub, N., Terris, M., et al. (COVID 2022,2). Effect of community and socio-economic factors on cardiovascular. ,*cancer and cardio-oncology patients with COVID-19.*, pgs 350-368.

5. Betti, M., N., B., Heffernan, J., & Raad, A. (2021). Could a NEW COVID-19 Mutant Strain Undermine Vaccination Efforts? A Mathematical modelling approach for estimating the spread of B.1.1.7 Using Ontario, Canada as a Case Study Vaccine.
6. Bonhoeffer, R. M. (2000). Production of resistant HIV mutants during antiretroviral therapy. *Journal of Applied Mathematics*.
7. Byul Nim, E. K. (2020). Mathematical Model of COVID-19 Transmission Dynamics in South Korea: The Impact of Travel Restrictions, Social Distancing and Early Detection . *Journal of Maths MDPI Publishers*, pg 1-18.
8. Chable-Bessia, C., Neyret, A., Swain, J., Henaut, M., Merida, P., Gros, N., et al. (COVID 2022). Low selectivity indices of ivermectin and macrocyclic lactones on SARS-COV-2 . *Replication in Vitro*, pgs 60-75.
9. Cherono Pela, K. W. (2019). Modelling the Effects of Immune Response and Time Delay on HIV-1 in Vivo Dynamics in the Presence of Chemotherapy. *Mathematical Modelling and Applications.*, 1-7.
10. Cho, D.-H., & Choi, G. (COVID 2022,2). Atorvastatin Reduces Severity of COVID-19. *A Nationwide, Total Population-Based, case-control study*, pgs 398-406.
11. Elrashdy, F., E.M., & Uversky, V. (2022). On the safety of covid-19 convalescent plasma treatment: Thrombotic and Thromboembolic concerns. *COVID 2022*, pgs 1-4.
12. Goudiaby M.S., G. L. (2022). Optimal control analysis of a COVID-19 and tuberculosis co-dynamics model. *Informatics in Medicine Unlocked.*, 1-28.
13. Kasia A Pawelek, S. L. (2012). A model of HIV-1 infection with two time delays: Mathematics analysis and comparison with patient data. *Journal of Mathematics Biology*, 98-109.
14. Kassahun Getnet Mekonen, S. F. (2022). Mathematical modelling and Analysis of Analysis of TB and COVID-19 coinfection. *Journal of applied mathematics Hindawi publishers*, pgs 1-20.
15. Kaur, A., C., M., Carpe, S., Congrete, S., Shahzad, H., Reardon, J., et al. (2022,2). Post-covid-19 . *condition and health status*, pgs 76-86.
16. Kotola BS, T. S. (2023). Bifurcation and Optimal control analysis of HIV/AIDS and COVID-19 co-infection model with numerical simulation. *PMCID*, 1-46.
17. Liu, T., Kang, L., Y., Huang, J., GUO, Z., Xu, J., et al. (2022). Simultaneous Detection of seven Human Coronaviruses by multiplex PCR and MALDI-TOFMS COVID. pgs 5-17.
18. Muthelo(2022), M. a. (2022 volume 36 number 2). COVID-19 and the Quality of mathematics education, teaching and learning in a first-year course. *South African Journal of Higher education*, pgs 189-203.
19. N. Ringa, M. L. (2022). HIV and COVID-19 co-infection: A mathematical model and optimal control. *Journal of informatics medicine Elsevier publishers*, pgs 1-17.

20. Ngina Purity M., R. W. (2017). Mathematical modelling of in vivo dynamics of HIV subject to the influence of the CD8+ T-cells. *Journal of Applied Mathematics*, 1153-1179.
21. O.Diekmann, J. (1990). On the definition and computation of R_0 in models for infectious diseases in heterogeneous populations. *Journal of Mathematical Biology*,, pgs 365-382.
22. Omame A, S. N. (2021). Analysis of COVID-19 and comorbidity co-infection model with optimal control. *Optim Control Appl Methods.*, 1568-1590.
23. Organisation, W. H. (2022). Enhancing Response of Omicron. SARS-COV-2 Variant. *Technical brief and priority actions for members states*, 1-28.
24. organization, W. H. (2020). Modes of Transmission of Virus Causing COVID-19 Implications for IPC Precaution recommendations. *WHO Scientific brief*, 1-3.
25. Otaki, J. N. (2022). Nonself mutations in the spike protein suggest an increase in the Antigencity and Decrease in the Virulence of the Omicron Variant of SARS-Cov-2. 407-418.
26. Pakwan Riyapan, S. E. (2021). A Mathematical Model of COVID-19 Pandemic A case study of Bangkok, Thailand. *Journal of Computational and Mathematical methods of medicine, Hindawi Publishers*, 11 pages.
27. Perelson, S. (1989). modelling the interaction of immune system with HIV in mathematical and stastical approaches to AIS epidemiology. *Journal of Mathematical and Statistics Appraoches on AIDs Epidemiology*, 350-370.
28. Peronace, C., Talerico, R., Colosimo, M., Panduri, G., Pintomalli, L., R., O., et al. (COVID 2022,2). B A.I Omicron Variant of SARS-COV-2. *First Case Reported in Calabria Region,Italy*, pgs 211-215.
29. Purnachandra., T. S. (2022). HIV/AIDS-Pneumonia Codynamics Model Analysis with Vaccinationand Treatment. *Computation and Mathematical methods in Medicine*.
30. Rahim Ud Din. Kamal Shah, I. A. (2020). Study of transmission dynamics of novel COVID-19 by using mathematical modelling. *Journal of Advance in Differnce Equations, Springer open publishers*, pgs 1-13.
31. Ringa N., D. M. (2022). HIV and COVID-19 co-infection: A mathematical model and optimal control. *Informatics in medicine unlocked.*, 1-17.
32. Sarbaz H.A. Khoshnaw, R. H. (2020). Mathematical Modelling for Coronavirus Disease (COVID-19) in Predicting future behaviors and sensitivity analysis. *Journal of Mathematical Modelling of Natural Phenomena*.
33. Schlickeiser, R., & Kroger, M. (COVID 2022,2). Forecast of Omicron . *Wave Time Evolution.*, pgs 216-229.
34. Viona Ojiambo, M. K. (2020). A Human-pathogen SEIR-P Model for COVID-19 Outbreak Under different intervention Scenario in Kenya. *Journal of Mathematics* , pgs 1-10.

35. W.R. Mbogo, L. (2013). Stochastic model for in-host HIV dynamics with therapeutic intervention. *Journal of Mathematical Biology*, 11.

UNDER PEER REVIEW